Dual Thermo- and pH-responsive Behavior of Double Zwitterionic Graft Copolymers for Suppression of Protein Aggregation and Protein Release

*Dandan Zhao, Robin Rajan and Kazuaki Matsumura**

School of Materials Science, Japan Advanced Institute of Science and, Technology, 1-1 Asahidai, Nomi, Ishikawa 923-1292, Japan

KEYWORDS: dual thermo-responsive, pH responsive, polyampholyte, protein aggregation, protein release

ABSTRACT: Graft copolymers consisting of two different zwitterionic blocks were synthesized via reversible addition fragmentation chain transfer polymerization. These polymers showed dual properties of thermo- and pH-responsiveness in an aqueous solution. Ultraviolet-visible spectroscopy and dynamic light scattering were employed to study the phase behavior under varying temperatures and pH values. Unlike the phase transition temperatures of other graft copolymers containing non-ionic blocks, the phase transition temperature of these polymers was

easily tuned by changing the polymer concentration. Owing to the biocompatible and stimuli-responsive nature of the polymers, this system was shown to effectively release proteins (lysozyme) while simultaneously protecting them against denaturation. The positively charged lysozyme was shown to bind with the negatively charged polymer at the physiological pH (pH 7.4). However, it was subsequently released at pH 3, at which the polymer exhibits a positive charge. Protein aggregation studies using a residual enzymatic activity assay, circular dichroism, and a Thioflavin T assay revealed that the secondary structure of the lysozyme was retained even after harsh thermal treatment. The addition of these polymers helped the lysozyme retain its enzymatic activity and suppressed its fibrillation. Both polymers showed excellent protein protection properties, with the negatively charged polymer exhibiting slightly superior protein protection properties to those of the neutral polymer. To the best of the authors' knowledge, this is the first study to develop a graft copolymer system consisting of two different zwitterionic blocks that shows dual thermo- and pH-responsive properties. The presence of the polyampholyte structure enables these polymers to act as protein release agents, while simultaneously protecting the proteins from severe stress.

INTRODUCTION

Stimuli-responsive polymers have attracted great attention in recent years. They respond to small changes in the surrounding environment, which makes them suitable candidates for applications in nanotechnology and biomedicine, for use as drug carriers[1–5] and smart surfaces,[6–9] and for protein separation.[10,11] However, as the field of applications expands, a single stimuli-responsive polymer can no longer fulfil the demands of the growing industry.[12] Therefore, the synthesis of

multi-stimuli-responsive polymers has become necessary. Compared with single-stimuli-responsive polymers, multi-stimuli-responsive polymers have additional properties that not only widen the applicability of polymers, but also allow for better control over the polymer conformation.[13]

Among the various stimuli-responsive polymers reported to date, thermo- and pH-responsive polymers have attracted the most attention.[12, 14] Thermo-responsive polymers can be classified into two types: systems exhibiting lower critical solution temperature (LCST)[15] and upper critical solution temperature (UCST) phase separations. Further, pH-responsive polymers have gained relevance because there is a difference in pH between human organs, normal tissue, and diseased tissue (e.g., the stomach, normal tissue, and a tumor have pH values of 1–2, 7.4, ~6.5, respectively).[16] pH-responsive polymer systems can be developed as drug delivery systems and gene delivery systems in vivo.

Therefore, in this study, we focused on the synthesis of graft copolymers that exhibit dual-thermo- and pH-responsive properties and attempted to control the phase transition temperature by changing the molecular mass and the concentration of the polymers.

For dual-thermo-responsive copolymers, the Poly (N-isopropylacrylamide)-poly-sulfobetaine (PNIPAM-PSPB) system has been widely studied. For instance, in our previous research[17], we showed that nanogels made of a copolymer of NIPAM and SPB show dual thermo-responsive reversible properties and exhibit swelling and shrinking with changing temperature. Additionally, Papadakis and his group reported a series of studies on the relationship between temperature and the shape of PNIPAM-PSPB micelles.[18–20] It is well known that PNIPAM shows LCST, and its transition temperature is observed near the physiological temperature. However, PNIPAM has several shortcomings, including non-biodegradability, inflammation, and activation of platelets

when it makes contact with blood.[21, 22] Moreover, the LCST is independent of the molar mass and concentration of the polymer, thus limiting the tunability of its properties by molecular design.[23] Further, PNIPAM does not exhibit a pH-responsive property, owing to its lack of ionic groups.

In a previous work, we reported that poly-L-lysine (PLL)-based polyampholyte, COOH-PLL, shows an LCST type of phase separation, which can be easily controlled by molecular design.[24] PLL is extensively used as a food additive due to its low toxicity.[25] Moreover, PLL can be degraded by amidases.[26] When the NH_2 group of PLL reacts with anhydrides such as succinic anhydride (SA), PLL transforms into an ampholyte molecule with both cationic and anionic moieties and thus exhibits both LCST and pH-responsive properties. Moreover, the LCST behavior can be easily tuned by optimizing charge balance, hydrophobicity, polymer concentration, and so on. Interestingly, COOH-PLL shows excellent cryoprotective properties[27] with various cells. Furthermore, it has been reported that polyampholyte exhibits antibiofouling properties.[28, 29] In addition, hydrophobically modified poly-L-lysine polyampholyte has been shown to deliver proteins at low temperatures.[30]

Unlike LCST, UCST has not been reported to occur in many polymers. Among the polymers showing UCST, poly-sulfobetaine (PSPB) has been frequently used. The UCST behavior of PSPB was found to be highly dependent on the molar mass and the concentration of the added low-molar-mass salts.[19] Because of its unique chain structures and high biocompatibility,[31] PSPB has been associated with unique properties such as cryopreservation[32] and has been used for anti-bio adherent coatings.[33] Moreover, in a previous work, we found that this polyampholyte exhibits a protein aggregation inhibition property, owing to its weak and reversible interaction with protein molecules, thereby acting as a molecular shield.[34–36] This phenomenon enables PSPB to assist proteins in the retention of their secondary structures and suppresses fibrillation of the protein,

even under severe stress. To utilize this kind of dual thermo-responsive polymer for biomedical applications such as protein delivery, PSPB was chosen along with COOH-PLL in this study for the graft polymer system.

The use of functional proteins in disease therapy has a long history. However, the development of protein therapeutics is limited, owing to protein instability. The misfolding and aggregation of the therapeutic protein reduces its treatment efficiency and even causes adverse reactions. For the advancement of the protein biopharmaceutics field, the development of newer systems that can protect proteins from unfolding and denaturation during delivery transport or under stress is of paramount importance. Moreover, the development of controlled and triggered release systems has caught the attention of researchers worldwide. In this work, we used reversible addition fragmentation chain transfer (RAFT) polymerization to develop graft copolymers consisting of two zwitterionic blocks, i.e., PLLSA-g-PSPB. The presence of the PLLSA segment allows these graft copolymers to exhibit LCST and pH-responsive properties and the PSPB block allows for UCST-type transition. Furthermore, we studied the phase behavior of these graft copolymers at different temperatures and pH values. Then, because of their pH-responsive properties, we used these graft copolymers as a protein release vehicle.[37] Electrostatic interaction provides a weak and reversible bond between the polymer and protein. Previous reports have suggested that polymer-protein hybrids can also be formed in such systems by self-assembly in aqueous solution.[38–45] Due to the presence of PSPB, the proteins were efficiently protected, even under severe conditions. To the best of our knowledge, the PLLSA-g-PSPB system proposed in this study, which consists of two different ampholytic segments and shows both dual thermo- and pH-responsive properties, is the first such system. Furthermore, the ability of the system to suppress protein aggregation and help proteins retain their secondary structures is noteworthy.

MATERIALS AND METHODS

Materials. Sulfobetaine monomer was donated by Osaka Organic Chemical Ind., Ltd. (Osaka, Japan) and used without further purification. A 25% (w/w) ε-poly-L-lysine (PLL) (molecular weight 4000) aqueous solution was purchased from JNC Corp. (Tokyo, Japan). Succinic anhydride (SA), 1-ethyl-3-(3-dimethylaminopropyl) carbodiimide hydrochloride (EDC-HCl) and N-Hydroxysuccinimide (NHS) were purchased from Wako Pure Chemical Ind., Ltd. (Osaka, Japan). 2-(dodecylthiocarbonothioylthio)-2-methylpropinic acid (RAFT agent), 4,4'-azobis-(4-cyanovaleric acid) (V-501, initiator), Thioflavin T (ThT), Micrococcus lysodeikticus and lysozyme from chicken egg white were purchased from Sigma-Aldrich (St. Louis, MO).

Synthesis of carboxylated poly-l-lysine (PLL-SA). PLL-SA with two different substitutions was synthesized. PLL-SA in which 50 mol% and 65 mol% of the amino groups were converted into COOH by the addition of SA were denoted as PLLSA50 (neutral at pH 7) and PLLSA65 (negative at pH 7), respectively. PLLSA50 was synthesized by adding succinic anhydride (9.76 mmol) to the 25% (w/w) ε-poly-l-lysine (PLL) aqueous solution (10 ml), followed by stirring at 50 °C for 1 h. Similarly, PLLSA65 was synthesized by dissolving succinic anhydride (12.67 mmol) in the 25% (w/w) ε-poly-l-lysine (PLL) aqueous solution (10 ml) followed by stirring at 50 °C for 1 h. After the reaction, the products were dried in an oven overnight and vacuum-dried for 1 day.

Synthesis of Macro-CTA (PLLSA-RAFT agent). We prepared two types of macro-CTA (PLLSA-RAFT agent): PLLSA50-RAFT agent and PLLSA65-RAFT agent. EDC (0.043 mmol), NHS (0.043 mmol), 2-(dodecylthiocarbonothioylthio)-2-methylpropionic acid (0.011 mmol) and 5 mL DMSO were added to a vial and stirred at 80 °C for 2 h. In another vial, 0.33 mmol PLLSA50 or PLLSA65 was dissolved in 10 mL DMSO at 130 °C. After 2 h, the two solutions were mixed together and reacted at 130 °C for 24 h. The polymer was purified by dialysis against water for 3 d using a dialysis membrane (MWCO 3.5 KDa, Repligen Corp. Waltham, MA, US). After dialysis, the polymer was obtained by lyophilization.

Synthesis of a graft copolymer of PLLSA and SPB (PLLSA-g-PSPB). The graft copolymers were synthesized using the following mixture ratio: [SPB monomer]:[V-501]:[macro-CTA] = 1000:1:5. PLLSA50-b-PSPB and PLLSA65-b-PSPB were synthesized by dissolving the SPB monomer (6.6 mmol), V-501 (6.6 μmol), and Macro-CTA (PLLSA50-RAFT and PLLSA65-RAFT agents, respectively) (33 μmol) in water (45 mL). The mixture was purged with nitrogen gas for 1 h and then stirred at 70 °C for 24 h. To study the kinetics of this reaction, the samples were removed from the reaction mixture at regular intervals, and ^{1}H NMR was used to monitor the disappearance of alkene protons during the course of the reaction. The polymer was then purified by dialysis against water for 3 d using a dialysis membrane (MWCO 14 KDa). After dialysis, the polymer was obtained by lyophilization.

Polymer characterization. The structural analyses of all polymer structures and time-dependent NMR were conducted on a 400 MHz Bruker Avance III spectrometer. The data was analyzed by NMR using the Topspin 3.5 software. The number of repeating units of the graft copolymers was

estimated by ^{1}H NMR from the relative area of the two peaks at around 4 ppm (corresponding to the α-protons of the substituted and unsubstituted PLL repeating units) and that of the poly-SPB peak at around 2.2 ppm. The numbers of NH_2 groups were determined by a 2,4,6-trinitrobenzene sulfonic acid (TNBS) assay.[46] In the TNBS assay, glycine was used as the standard solution. A solution containing 0.3 ml of 250 μg/mL of solution, 1 mL 0.1% (w/v) of TNBS solution, and 2 ml of a solution containing 4% (w/v) $NaHCO_3$ and 10% (w/v) sodium dodecylsulfate was prepared. The solution was then incubated at 37 °C for 2 h. After the incubation, the absorbance of the sample solutions was measured at 335 nm using UV-vis spectroscopy (UV-1800, Shimadzu Corp., Kyoto, Japan).

Dynamic light scattering (DLS). A Zetasizer 300 system (Malvern Instruments, Worcestershire, UK) was used to determine the hydrodynamic diameter and the surface charge of the graft copolymers. The scattering angle was 173°. The thermo-responsiveness of the polymers was measured by DLS in temperature steps of 2 °C with three measurements per temperature.

Ultraviolet–visible (UV-Vis) spectroscopy for the determination of thermo- and pH-responsive properties. The turbidity of the graft copolymers was determined by UV-visible spectroscopy (UV-1800, Shimadzu Corp., Kyoto, Japan) at 550 nm. Each transmittance value was obtained at a different temperature, and there was a 12 min stabilization period at every temperature.

Transmission electron microscopy (TEM). The morphology of the graft polymer was observed using a TEM H-7650 instrument (Hitachi, Tokyo, Japan). The sample was first dissolved

in distilled water (0.1%) and 5 μL sample solution was placed on a copper grid (NS-C15 Cu150P; Stem, Tokyo, Japan). After drying at different temperatures (4 °C and 70 °C), the grid was negatively stained with 1% phosphotungstic acid (Sigma Aldrich, Steinheim, Germany) for 30 s, washed with one drop of distilled water, and air-dried.

Protein release experiment. A polymer solution (6% (w/w)) and lysozyme solution (2% (w/w)) were prepared in phosphate-buffered saline (PBS, pH 7.4). Following this, the polymer and lysozyme solutions were mixed and incubated for 2 h at 25 °C. After the incubation, the samples were centrifuged for 2 h at 13.2 × 1000 rpm (15 °C) using 30K MWCO centrifugal filter devices. The solution was separated into two parts. A PBS solution appeared in the filtrate collection tube with the non-bound lysozyme, whereas the protein that succeeded in binding with the polymer remained in the filter device. The liquid that appeared in the filtrate collection tube was checked for the non-bound lysozyme by the Bradford assay.[47] Lysozyme loading efficiency was calculated using the following equation.

$$\text{Protein loading efficiency} = \frac{Total\ amount\ of\ protein - Free\ protein}{Total\ amount\ of\ protein} \times 100\% \quad (1)$$

The concentrated solution containing polymer-bound protein, which was retained in the filter device, was diluted, and the pH was reduced to 3 by the addition of 1 M HCl solution. DLS was employed to measure the hydrodynamic radius of the polymer and that of the protein before and after the pH change.

Residual lysozyme activity. A lysozyme solution (20 μM) was mixed with polymer solutions (at various concentrations) in PBS (pH 7.4). Following this, the lysozyme-polymer solution was

heated at 90 °C for 30 min. After 30 min, a Micrococcus lysodeikticus (2 mL, 0.25 mg/mL in PBS) solution was mixed with 100 μL of the lysozyme-polymer solution. The transmittance of this mixture solution was measured by UV-vis spectrophotometry (UV-1800, Shimadzu) at 600 nm from 0 to 6 min with constant stirring. A continuous downward line was obtained. The slope of this line indicated the activity of the residual lysozyme.

Fibril formation of lysozyme. The fibril formation of the lysozyme after heating for 30 min at 90 °C was determined by a ThT assay. ThT binds to β-amyloid fibrils, which leads to an increase in fluorescence intensity.[48] First, the stock solution was prepared by adding 4 mg ThT to a 5 mL PBS solution (pH 7.4) followed by filtration with 0.22 μM filter. Following this, the working solution was prepared by adding 1 mL of the stock solution to 49 mL of PBS (pH 7.4). The lysozyme solution (40 μM) was mixed with an equal volume of the polymer solution. The lysozyme-polymer solution was then heated at 90 °C for 30 min with the final concentration of lysozyme being 20 μM and that of polymer being 1 %, 2.5 %, and 5 % (w/w). Following this, 100 μL of the lysozyme polymer solution was mixed with 2 mL of the ThT solution, and the fluorescence was measured by JASCO FP-8600 with an excitation wavelength of 450 nm and emission wavelength of 485 nm.

Circular dichroism (CD) spectroscopy. A CD spectropolarimeter (JASCO-820) was employed to monitor and determine the change in the secondary structures of the lysozyme before and after heating. A transparent quartz cuvette with a path length of 0.5 cm was used to measure the CD spectra. The final concentration of the lysozyme and polymer components in the lysozyme-

polymer solution was 20 μM and 5 % w/w, respectively. The scanning range was 190–320 nm with a bandwidth of 1 nm and scanning speed of 0.2 nm/s.

Cytotoxicity Study. L929 (American Type Culture Collection, Manassas, VA, USA) cells were cultured in Dulbecco's modified Eagle's medium (DMEM, Sigma-Aldrich, St. Louis, MO), supplemented with 10% heat-inactivated fetal bovine serum in a humidified atmosphere of 5% CO_2 at 37 °C. The cytotoxicity assay was performed according to the MTT method in a 96-well plate. Briefly, 1×10^3 cells in 0.1 mL of culture media were seeded in a 96-well plate. After incubation for 72 h, 0.1 mL of the culture medium, which contained different concentrations of the polymer, was added to the 96-well plate. After re-incubation for 24 h, 0.1 mL MTT (3-(4,5-dimethylthiazole-2-yl)-2,5-diphenyltetrazolium bromide) solution (300 μg/mL) was added to each well, and the cells were incubated for an additional 3 h. After discarding the media, 0.1 mL of DMSO was added to dissolve the purple formazan crystals that had formed. The absorbance values at 540 nm were determined using a microplate reader (versa max, Molecular Devices Co., CA, USA). The value of the absorbance indicated the number of viable cells.

RESULTS AND DISCUSSION

Polymer characterization. The graft copolymers were prepared by RAFT polymerization as shown in Scheme 1. Two graft copolymers with different degrees of substitution of SA in PLL were obtained. ^{1}H NMR and ^{13}C NMR spectroscopy were employed to characterize these polymers (Supporting Information). We can clearly identify the characteristic peaks of the two segments in Figure S1. The degree of substitution (DS) of SA into PLL and the number of RAFT agents substituted per chain were determined by ^{1}H NMR (Figures S1 and S2) and the TNBS assay. The

obtained degree of substitution of SA was almost the same in the feeding condition (Table 1). Calculations based on the results of the TNBS assay and NMR spectroscopy clearly reveal that approximately 1 RAFT agent was substituted on the PLLSA chain (Table 1). Table 2 shows the molecular weights (M_n) of these polymers, which were calculated by NMR spectroscopy. P1 and P2 represent the copolymers PLLSA(50)-g-PSPB(200) and PLLSA(65)-g-PSPB(200), respectively. Here, 200 in the parenthesis after PSPB indicates the number of repeating units of SPB. The degree of polymerization of SPB in P2 was higher than that of P1. Figures S3–S6 show the ^{1}H- and ^{13}C-NMR charts for P1 and P2.

Scheme 1. Schematic illustration of the synthesis of PLLSA-g-PSPB.

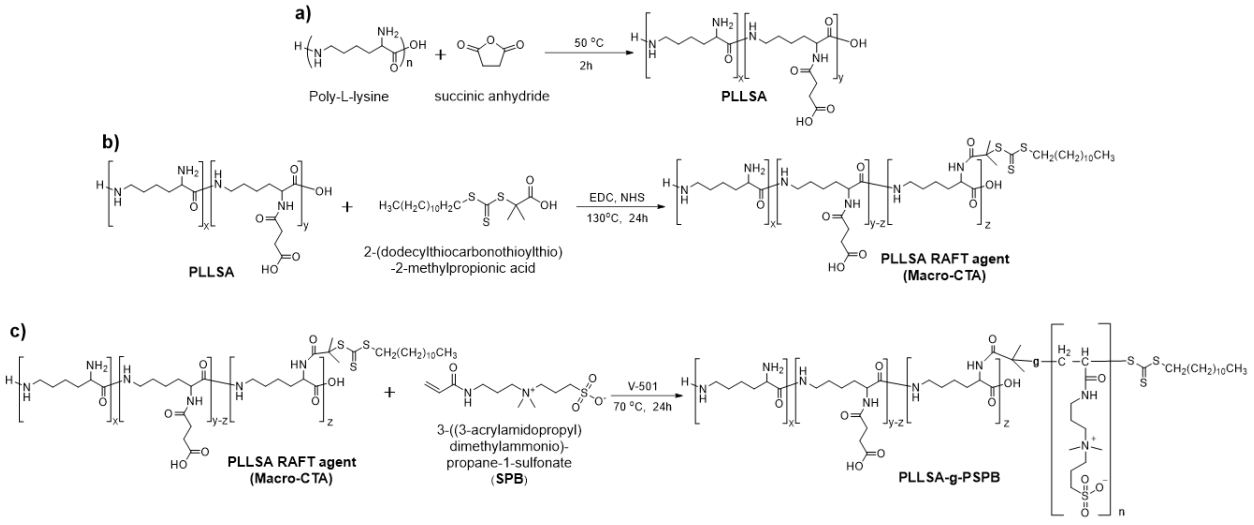

Table 1. Characteristics of the macro-chain transfer agent (CTA)

Polymer		DS[b]		Number of NH_2[c]	Number of RAFT agents substituted per chain[e]	
		TNBS[c]	NMR[d]		TNBS[c]	NMR[d]
PLLSA50	In feed	50%		16.73	-	-
	In polymer[a]	46.5%	47%			

PLLSA50 RAFT Agent	In feed	-	15.68	1.05	0.95
	In polymer[a]				
PLLSA65	In feed	65%	10.72	-	-
	In polymer[a]	65.7% 63.6%			
PLLSA65 -RAFT Agent	In feed	-	9.52	1.20	1.25
	In polymer[a]				

Note: [a] Determined by ^{1}H NMR. [b] Degree of substitution (DS) of SA into PLL. [c] Calculated by the TNBS assay (PLL has ~31 repeating units). [d] Determined by ^{1}H NMR. [e] Determined by subtracting the number of NH_2 in PLLSA from the RAFT agent substituted PLLSA.

Table 2. Characteristics of graft copolymers prepared via RAFT polymerization

Entry	Polymer[a]	Number of repeating units			Molar ratio[c]	$M_n \times 10^{-3}$ [b]
			PLLSA	PSPB		
P1	PLLSA(50)-g-PSPB200	In feed	31.25	200	1000:1:5	41.1
		In polymer[b]	31.25	125.4		
P2	PLLSA(65)-g-PSPB200	In feed	31.25	200		58.0
		In polymer[b]	31.25	181.5		

Note: [a]Number in parenthesis next to PLLSA indicates the % substitution of SA in PLL and the subscript next to PSPB denotes the degree of polymerization of SPB. [b] Determined by ^{1}H NMR. [c][Monomer]:[Initiator]:[RAFT agent] (monomer: SPB, initiator: V-501, RAFT agent: PLLSA-RAFT agent).

Time-dependent ^{1}H NMR was used to determine the conversion of SPB in the RAFT polymerization and to study the kinetics of RAFT polymerization. Completion of the reaction was monitored by observing the loss of vinyl protons from the monomer (Figure S7 and Figure S8). The relationship between $\ln([M]_o/[M])$ and time is shown in Figure S9. An almost linear first-order

kinetic plot was obtained, suggesting that the reaction follows living polymerization kinetics. After 3 h, the reaction was nearly 70% complete.

Dual-thermoresponsive Property. Figure 1 shows photographs of an aqueous solution containing 1 wt. % of P2 taken at different temperatures. The solution was transparent at 40 °C, while it was turbid at 4 °C and 70 °C. The pictures clearly show that heating and cooling lead to changes in the solubility of the polymer. This result clearly indicates that this graft copolymer exhibits LCST- and UCST-type phase separation properties.

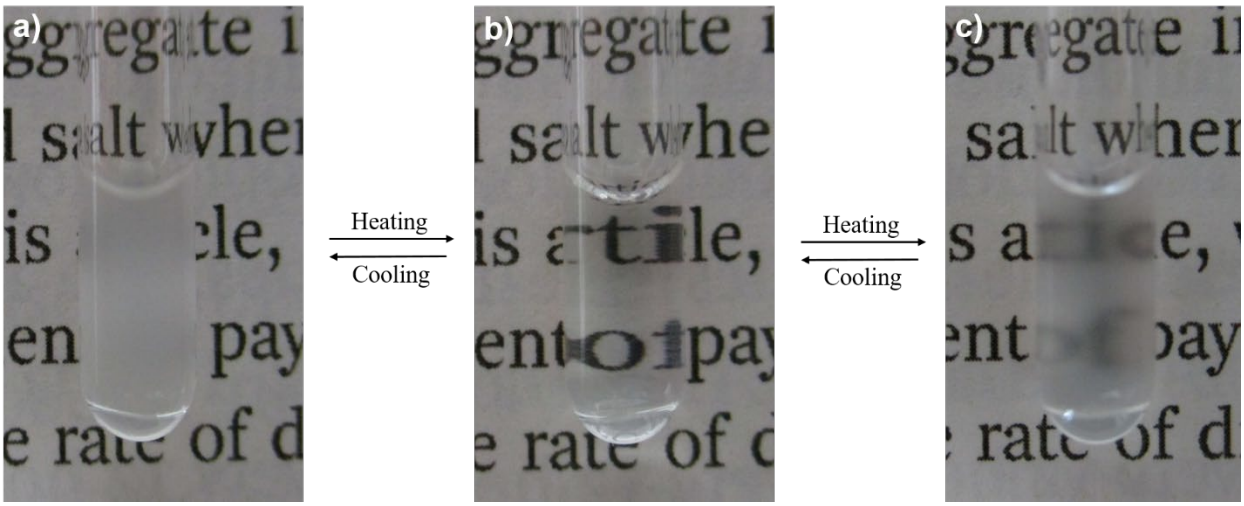

Figure 1. Photographs of the graft copolymer (P2, 1% w/w) before and after cooling. The photographs (a), (b), and (c) were taken at 4 °C, 40 °C, and 70 °C, respectively.

The thermoresponsive property of the graft copolymers was determined by turbidimetry in water by UV-vis spectroscopy at a 550 nm wavelength. Figure 2 shows the phase transition behavior of P1 and P2 at different concentrations. Each of the graft copolymers display both LCST- and UCST-type phase separation behavior. With an increase in temperature, the polymer solution undergoes insoluble-soluble-insoluble transition. Upon heating, the transmittance of the solution increases

and as the temperature is further increased, the transmittance of the solution starts decreasing. At low temperatures, the graft copolymer (SPB segment) exhibits UCST-type transition, and at high temperatures, the graft copolymer (PLLSA segment) exhibits LCST-type transition. For P1 (Figure 2a), at 14 °C, the polymer solution is turbid, and the transmittance increases with the temperature. When the temperature reaches 40 °C, the transmittance reaches its maximum value. However, as the temperature increases beyond 44 °C, the transmittance starts decreasing. From around 46 °C to 80 °C, the polymer exhibits LCST behavior (PLLSA segment). The transmittance decreases with further increases in temperature because of the gradual dehydration of the PLLSA chain (LCST transition). Similarly, in the case of P2 (Figure 2b), the transmittance of the solution increases when the temperature increases from 16 °C to 46 °C. This is followed by a decrease in transmittance with further increases in the temperature, up to 80 °C. Figure 2 clearly shows that the polymer exhibits both a UCST and a LCST behavior. In addition, we observe that the slope of the curve corresponding to a UCST behavior is larger than that corresponding to a LCST behavior; this is because the graft copolymer contains more UCST segments than LCST segments, i.e., more repeating units of PSPB are present as compared to those of PLLSA (Table 2). Meanwhile, the electrostatic interaction between the PSPB chain and PLLSA chain might affect the speed with which the transmittance decreases.

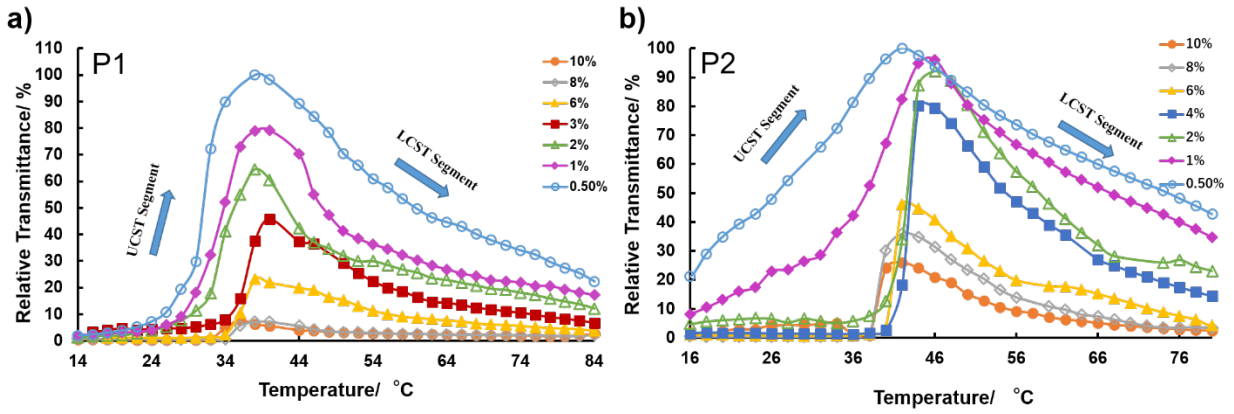

Figure 2. Relative transmittance of polymer solutions of (a) P1 and (b) P2 at various concentrations.

The phase diagram for the graft copolymers was plotted by gathering the points at which the transmittance reaches half of its maximum value. From Figure 3, we can see that the phase separation temperature was affected by both the degree of polymerization of the SPB and the degree of the substitution of SA in PLL. The cloud points of P1 were slightly higher than that of P2 because in P2, the degree of polymerization of the SPB was higher than that of P1. This result is consistent with the results shown in Figure 2. The UCST increases because an increase in M_n leads to a decrease in the mixing entropy.[49] The LCST of P2 is higher than that of P1; this result is also consistent with those of previous studies.[24] Because PLLSA50 contains an equal number of amino and carboxyl groups, the interactions between the two groups is stronger than that of PLLSA65; hence, P1 shows phase separation at lower temperatures. Figure S10a and Figure S10b show the phase diagrams of the PSPB and PLLSA homopolymers. For the PSPB homopolymer (Figure S10a), the cloud points of the PSPB homopolymer increased with increasing concentration, indicating a similar trend observed in Figure 3. Figure S10b shows the phase diagrams of the PLLSA50 homopolymer. Compared to the graft polymer, we found that, after grafting PSPB on the PLLSA, the cloud points of the PSPB and PLLSA are higher than those of the homopolymers. The increase in cloud points is possible due to the PLLSA segment acting as a hydrophilic segment at the temperature lower than the LCST and the PSPB segment acting as a hydrophilic segment at the temperature above the UCST. This corresponds well with the understanding that the addition of a hydrophilic segment increases the phase transition temperature.[24] Figure S10c shows the hysteresis curves of P1 at 2% concentration. These curves were achieved by measuring the

transmittance on first increasing the temperature gradually until 70 °C followed by cooling. Very small hysteresis on heating and cooling cycles was observed from the curves.

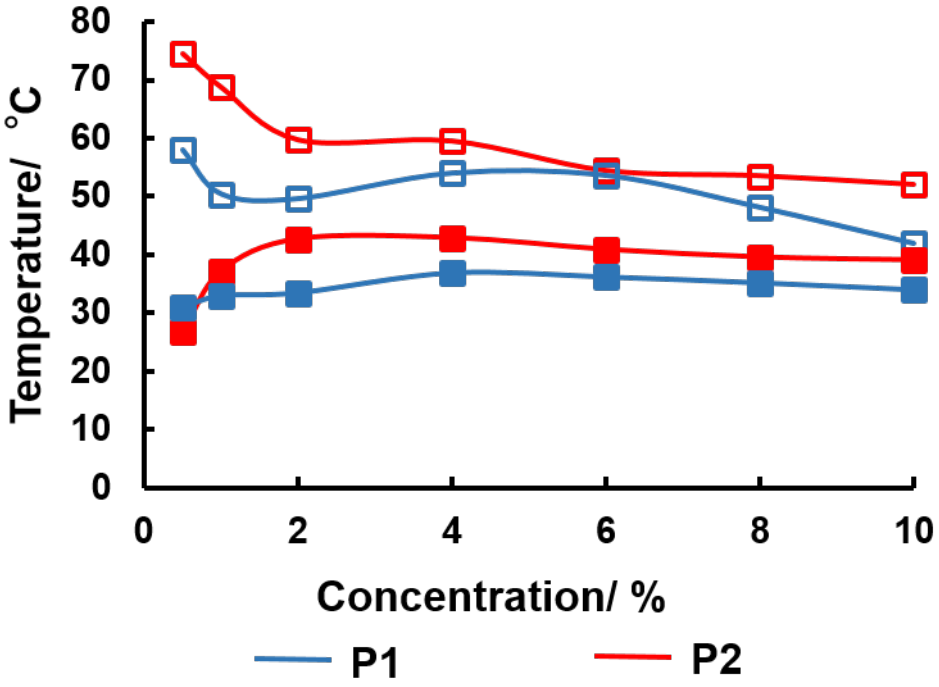

Figure 3. Phase diagram of the polymer solutions of P1 and P2; the open squares represent LCST transitions and the closed squares represent UCST transitions.

The size of these graft copolymers was then studied using DLS 0.75% (w/w). As shown in Figure 4, at lower and higher temperatures, the size of the polymers aggregates was larger than those at medium temperatures (around 30–40 °C), indicating that at lower and higher temperatures, the SPB segment and PLLSA segments aggregated. This result also corresponds well with the result obtained by UV-Vis spectroscopy. Moreover, the PLLSA segments aggregate at higher temperatures, which is why the polymer shows larger size aggregates. The size of the polymer aggregates at high temperature is larger than that at low temperature.

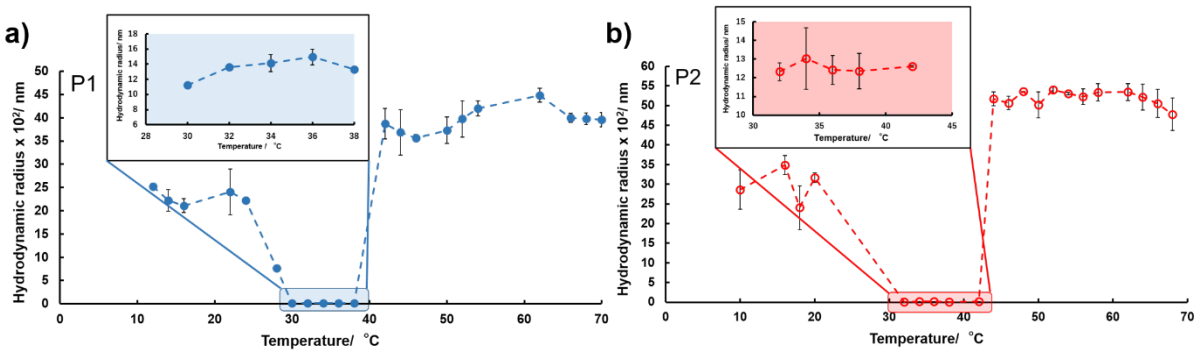

Figure 4. Temperature-dependent DLS measurements of the graft copolymer in water at a polymer concentration of 0.75 % for a) P1 and b) P2.

Further, the morphology of the graft polymer was studied by TEM of P1 and P2, which were dried at different temperatures. Figure S11 shows the TEM images of the graft polymer at 0.1% concentration. When dried at 4 °C, which is lower than the UCST (Figure S11a and Figure S11c), the diameter of these graft polymers was around 80 nm and the size showed a broad distribution. At this temperature, the graft polymer may have formed a core-shell micelle with PSPB acting as the core and PLLSA as the shell. On the other hand, when the sample was dried at 70 °C, which is higher than the LCST (Figure S11b and Figure S11d), the diameter of these graft polymers was around 50 nm. At this temperature, the graft polymer may have again transformed into a core-shell micelle with PLLSA acting as the core and PSPB as the shell.

pH-responsive Property. The pH-responsive property was investigated by UV-Vis spectroscopy by measuring the change in transmittance with the change of pH. Figure 5 shows that the transmittance increased with an increase or decrease in the pH of the solution. At pH 1 and pH 13, the transmittance achieved its maximum value. Following pH change, more H^+ or OH^- were added

into the solution, which affected the hydrogen bonds or the electrostatic interaction in PLLSA and in SPB, resulting in the solution changing from turbid to transparent.

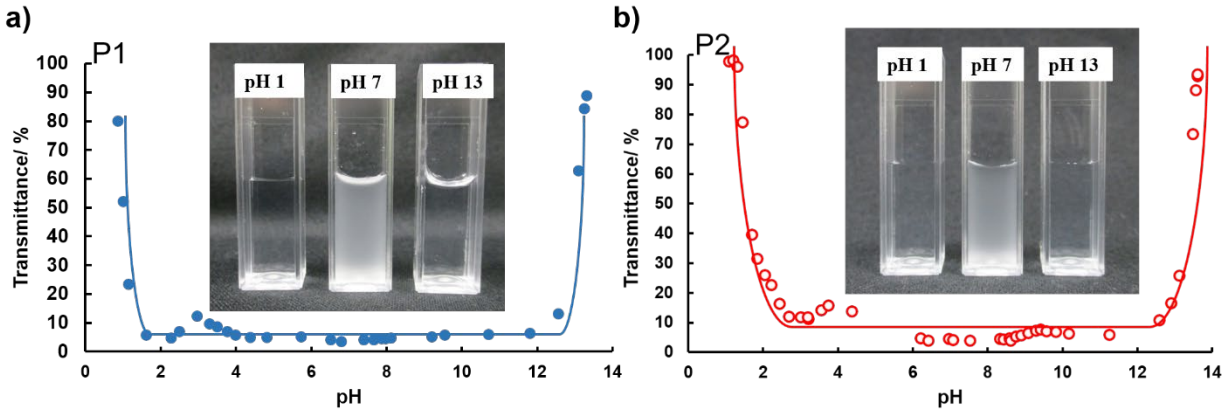

Figure 5. Relative transmittance of polymer solutions of (a) P1 (1% w/w) and (b) P2 (1% w/w) at various pH values.

Figure 6 shows the zeta potential results of the graft copolymers at different pH values. Because P2 contains negatively charged PLLSA (65), the zeta potential is more negative than that of P1. Moreover, at ~pH 7, both P1 and P2 exhibit negative charges, and with a decrease in the pH, the zeta potential of these polymers becomes positive. This interesting property can be potentially used to deliver any positively charged protein or drug, and we exploited this property to release a positively charged protein in this study. The isoelectric point calculated by the pH at which zeta potential becomes neutral is 5.5 for P1 and 4.6 for P2.

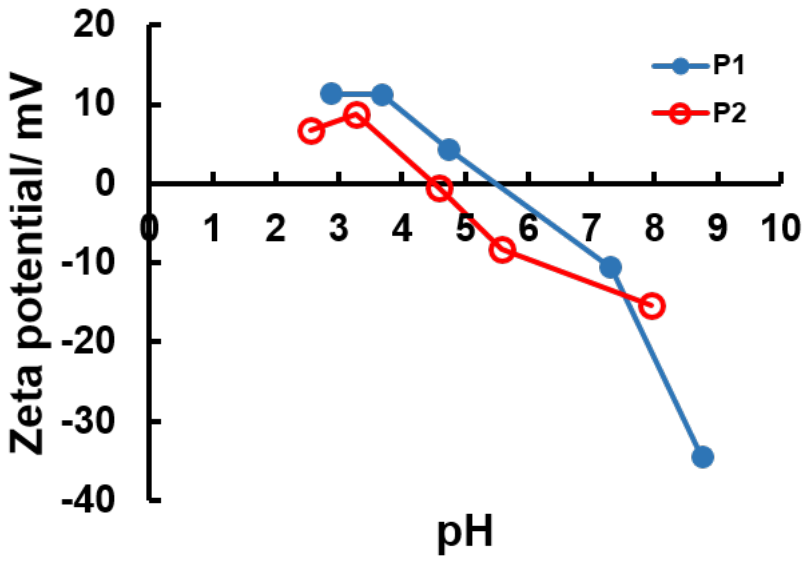

Figure 6. Measurement of the zeta potentials of the polymer solutions of P1 (1% w/w) and P2 (1% w/w) at different pH values.

Protein release. A positively charged protein can be bound to a negatively charged polymer via electrostatic interaction. As can be seen from the results above, when the pH value of the polymers was 3, the charge of the polymers changed from negative to positive; therefore, if a positively charged protein is bound to such a polymer at the physiological pH, the protein can be released owing to electrostatic repulsion when lowering the pH. Lysozyme was chosen as the model protein for this study. This is primarily because of the net positive charge of this protein.[50] Moreover, its structural details have been studied extensively, and complete information about its higher order structures is known.[51, 52] For this study, the polymer and lysozyme were dissolved in PBS (pH 7.4) and then incubated at 25 °C for 1 h. The solution was then transferred to the centrifugal filter units with MWCO 30K and then centrifuged at 15 °C at 13.2 × 1000 rpm for 2 h. The solution at the bottom consisted of unbound lysozyme and the filter at the top retained the protein bound to the

polymer. The amount of unbound protein was quantified by a Bradford assay using the Bradford Ultra reagent (Expedeon Ltd., Harston, UK). By using equation (1), it was found that 94.25% of the protein was successfully bound to the polymer.

The protein release experiment was performed using DLS. The solution containing polymer-bound protein, which stayed on top, was collected, and the pH was changed to 3. DLS was employed to measure the hydrodynamic radius of the polymer and that of the protein before and after pH change. From Figure 7, we clearly see that a peak appeared around 1000 nm (blue line with open circles) after changing the pH to 3. Before changing the pH of the solution (pH 7.4), only one peak (yellow line with closed circles) was present, which indicated that the protein was completely bound with the polymer. However, the protein released showed slight aggregation, which may be due to the duration of the centrifugation.

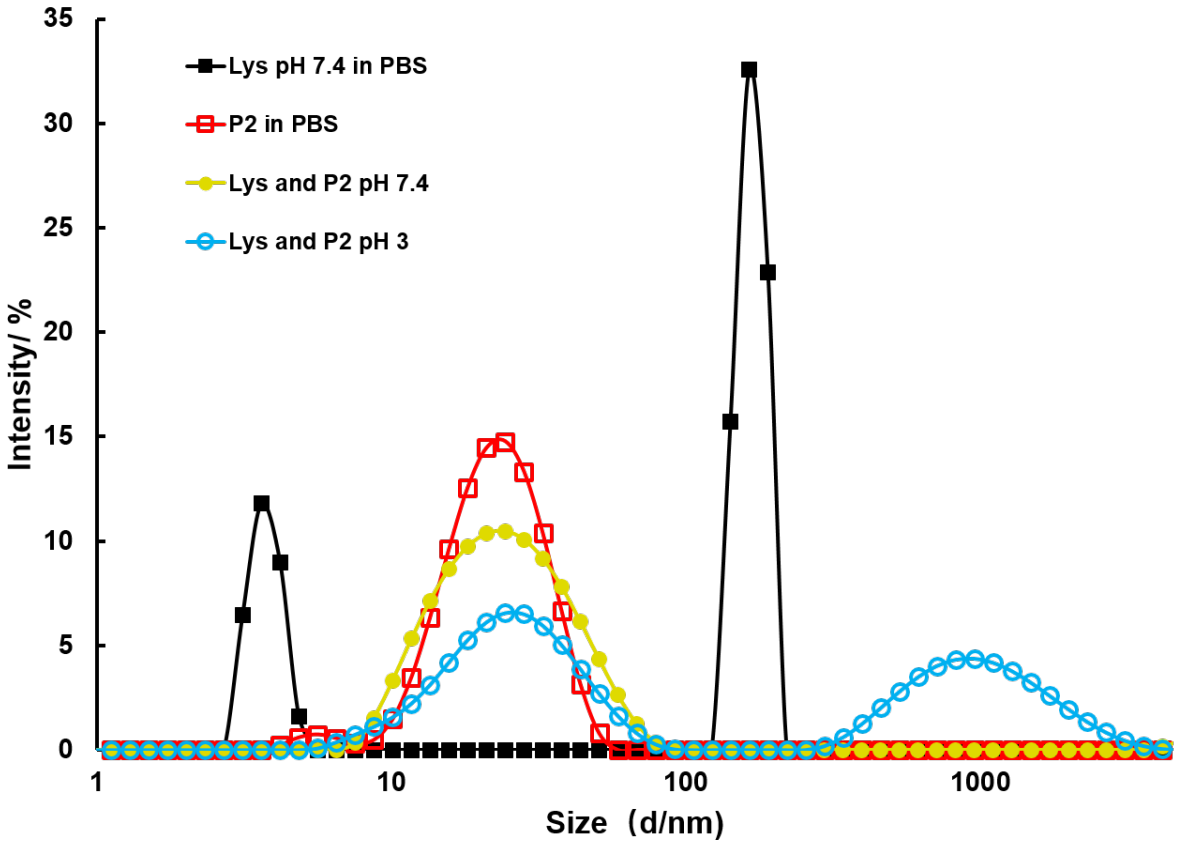

Figure 7. Particle size of the lysozyme polymer solution at different pH.

Protein aggregation inhibition. Figure 8 shows photographs taken after lysozyme treatment at 90 °C for 30 min with and without the polymer. The native lysozyme solution was obtained by dissolving lysozyme in PBS (pH 7.4, 1 mg/mL) (Figure 8a). A clear aggregation can be seen in Figure 8b; this photograph was taken after the lysozyme solution was heated at 90 °C for 30 min without the addition of any polymer. In contrast, when the lysozyme solution was heated at 90 °C for 30 min in the presence of 5% (w/v) P1 (Figure 8c) or P2 (Figure 8d), no significant aggregation could be seen. These results clearly show that P1 and P2 possess lysozyme aggregation inhibition properties. This may be due to the formation of polymer-protein hybrids (Figure S12).[53–56] To quantify the extent of aggregation and protection, and to investigate any changes in the higher-order structure of proteins on aggregation, further studies were conducted.

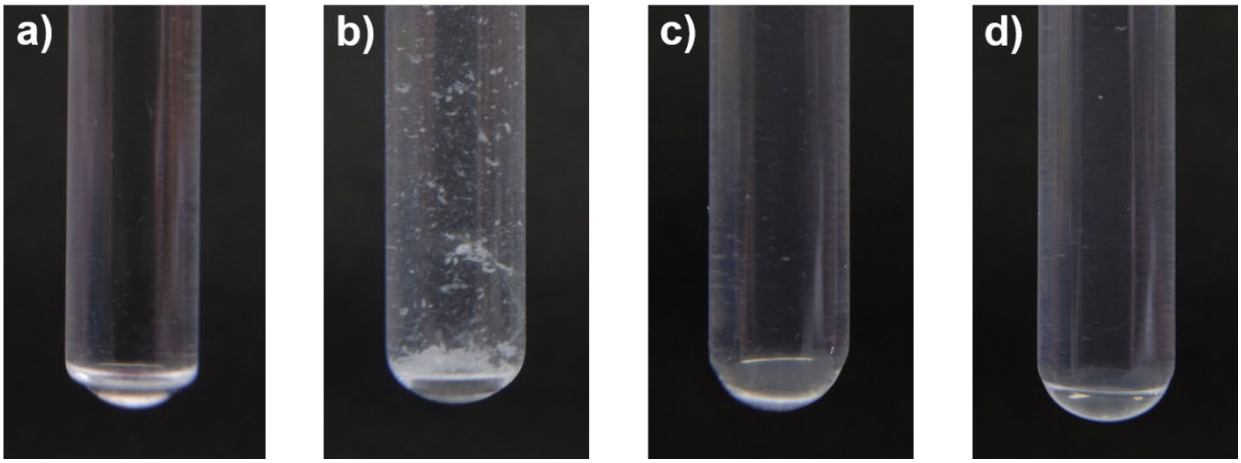

Figure 8. Photographs of lysozyme in PBS (1 mg/mL): a) native lysozyme; b) treatment at 90° C for 30 min without polymer presence; c) with 5% (w/w) of P1; and d) with 5% (w/w) of P2.

Amyloid Fibril Formation. Figure 9a shows the result of the fibril formation of lysozyme in the presence of different concentrations of the polymer after heating for 30 min at 90 °C. The ThT assay was used to determine the amount of the amyloid fibrils in solution. We found that when the

polymer concentration increased, the intensity of ThT fluorescence started decreasing. This clearly indicates that addition of the graft copolymer suppresses the formation of fibrils. The ThT fluorescence observed was less than 10% when 5% of P2 was present. In comparison with P1, P2 showed higher efficiency in suppressing the formation of amyloid fibrils. In this study, as P2 exhibits an overall negative charge, which enables a stronger interaction with the positively charged lysozyme, the formation of fibrils is suppressed to a greater extent than that by P1. Furthermore, it has been established that hydrophobic interaction plays an important role in protein fibril formation and also that ampholytic polymers act as molecular shields that reduce the formation of the fibrils.[34] Another possible explanation for the increased efficiency of P2 against fibril formation is the prevention of interactions between the hydrophobic domains of the protein owing to their electrostatic interactions with the polymer.

Residual Enzymatic Activity. To assess the proficiency of the graft copolymers in protecting proteins after heat treatment, we investigated the residual enzymatic activity of lysozyme. The enzymatic activity of lysozyme after heat treatment was investigated by the decrease in turbidity of a Micrococcus lysodeikticus cell suspension following the addition of lysozyme. Faster breakdown of the Micrococcus lysodeikticus cell suspension represents higher residual activity of lysozyme, indicated by a decrease in the turbidity of the solution, which was monitored by UV-Vis spectroscopy. From Figure 9b, we can clearly see that the activity of lysozyme is maintained in the presence of both P1 and P2. Nearly 70% of lysozyme remains active in the presence of a 5% concentration of P2. Compared with our previous work, these polymers exhibit more efficiency in protecting lysozyme than that of linear poly-SPB.[34, 57] The lysozyme protective property of P2 is higher than that of P1. This is in agreement with the results obtained with ThT, which revealed

that the negatively charged P2 interacted more strongly with lysozyme, leading to increased protection. Complete loss in activity was calculated by heating lysozyme solution without any additive and the percent residual activity was calculated relative to these values.

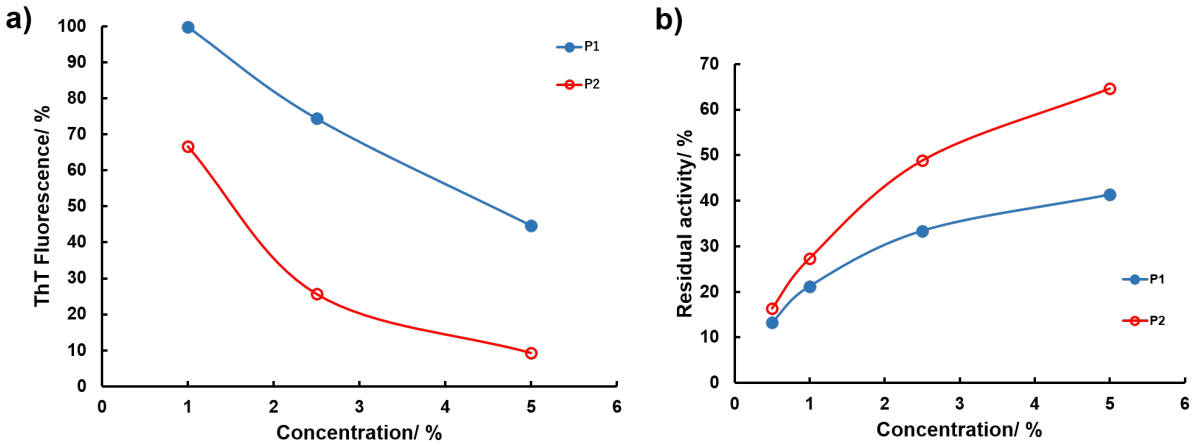

Figure 9. a) Analysis of fibril formation of lysozyme in the presence of different concentrations of polymers after treatment at 90 °C for 30 min as determined by the ThT fluorescence assay. b) Residual activity of lysozyme in the presence of different concentrations of polymers after treatment at 90 °C for 30 min. The activity was measured with a UV-Vis spectrophotometer.

CD Spectroscopy. The change in the secondary structure of the lysozyme was analyzed by CD spectroscopy. All collected data were the average of three scans and were measured in the presence of N_2 gas. As shown in Figure 10a, the CD spectra of native lysozyme without heating showed negative peaks near 205 nm and 220 nm, indicating the presence of the β-sheet and α–helix structure.[58] After heating for 30 min at 90 °C, the intensity of these peaks decreased significantly, indicating that high temperature leads to the loss of the α– helix and β-sheet structure (red line). However, after addition of the polymer (5% w/w), the negative peaks near 205 nm and 220 nm were retained with almost the same intensity as that observed with native lysozyme. This indicates that these graft copolymers help in the retention of the secondary structure of lysozyme. Further,

to confirm the ratio of each secondary structure element, the CDSSTR algorithm with the reference set 7 of the DichroWeb server was used to deconvolute the CD spectra.[59, 60] We observed the following secondary structure contents, as shown in Figure 10b: lysozyme without heating: 45% α– helix, 21% strand, 14% turn, and 21% unordered; lysozyme with heating: 5% α– helix, 28% stand, 18% turn, and 48% unordered. Considerable decrease in the α– helix content was seen after high temperature treatment, and this was compensated for by an increase in the amount of the unordered conformation. A slight increase in the β-strand was also observed. This clearly indicates that high-temperature treatment completely alters the higher structure of lysozyme. It is worth noting that, in the presence of 5% (w/w) P1 and P2, the fraction of the secondary structure elements did not show significant change compared with lysozyme without heating. Although a slight decrease in the α-helix portion was observed, almost all of the secondary structure of the lysozyme was retained in the presence of these graft copolymers. The ability of P2 to retain the secondary structure was slightly higher than that of P1, and this is consistent with the results obtained from the ThT assay and residual enzymatic activity. The retention of the higher-order structure of lysozyme in the presence of these graft copolymers stabilizes lysozyme and enables solubility in the buffer even after high temperature treatment, thus suppressing the aggregation of lysozyme.

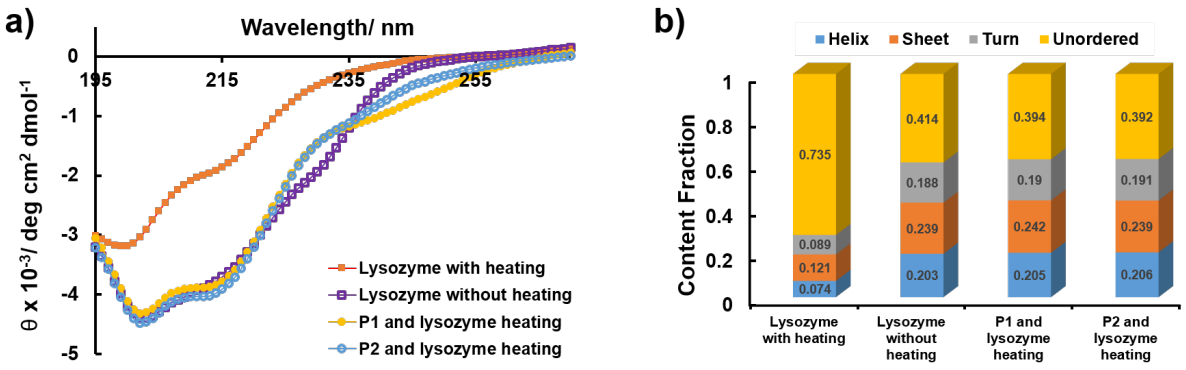

Figure 10. a) Representative far-UV CD spectra of lysozyme in the absence and presence of polymers (5% w/w) after incubation at 90 °C for 30 min. b) The contents of the secondary structure of lysozyme.

Cytotoxicity Assay. Figure 11 shows the cytotoxicity of the polymers, and the results clearly demonstrate that both P1 and P2 show very low toxicity, even at very high concentrations of the polymer (5% w/w), with cell viability observed to be greater than 60%. Usually, cytotoxicity is evaluated by the concentration of the test compound needed to kill half of the cells, IC_{50}. IC_{50} was not observed at these concentrations. Low toxicity indicates these polymers are extremely biocompatible and can be safely used in living organisms for various biomedical applications.

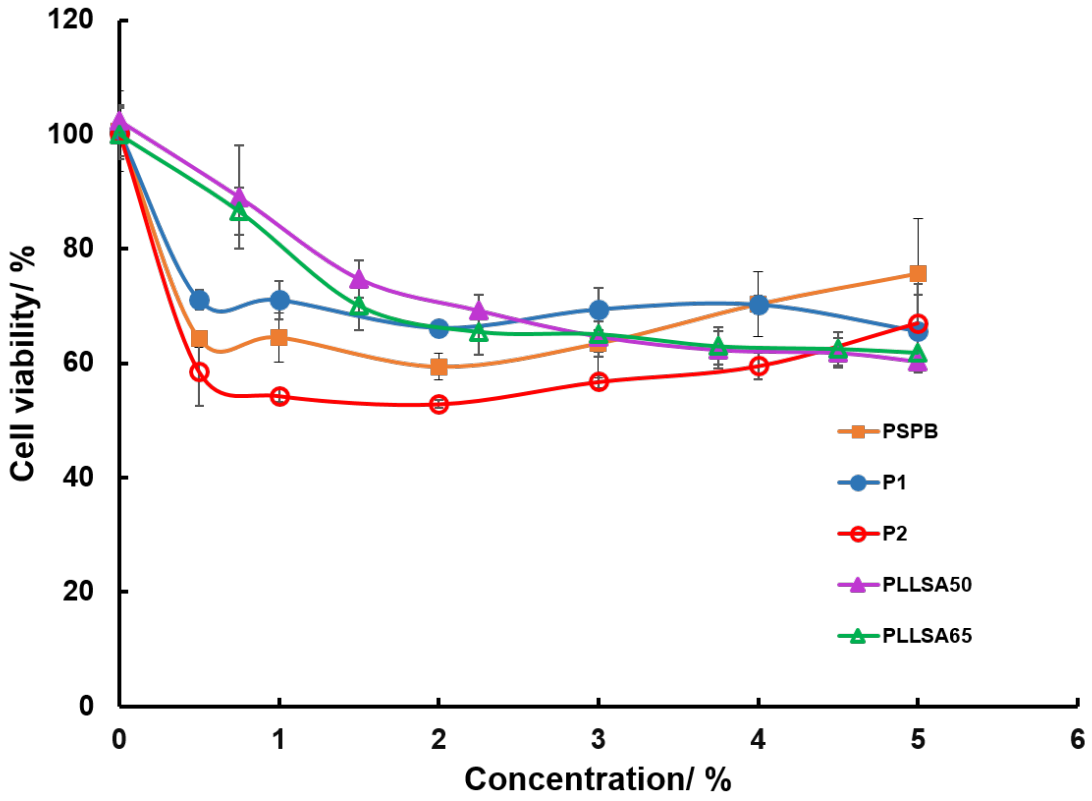

Figure 11. Cytotoxicity of the polymers. L929 cells were treated with different concentrations of polymers: PSPB (closed squares), P1 (closed circles), P2 (open circles), PLLSA50 (closed triangles), and PLLSA65 (open triangles).

CONCLUSIONS

In conclusion, two dual-thermo- and pH-responsive graft copolymers were successfully synthesized by RAFT polymerization. These graft copolymers contain two different polyampholyte segments. To the best of the authors' knowledge, this is the first study to use PLLSA as an LCST-inducing segment in a graft copolymer, thus imparting a new and interesting characteristic to the graft copolymer. The presence of two zwitterionic segments not only allows the graft copolymer to exhibit a dual-temperature responsive property, but also allows the polymer to exhibit a pH-responsive property. Interestingly, we found these polymers can have multiple functionalities, i.e., they can be used as a protein release vehicle and, at the same time, can suppress protein aggregation under severe stress. A very high protein protection efficiency was observed, with more than 70% of the activity being retained even after heating at very high temperatures, and the secondary structure of the lysozyme was also retained in the presence of these graft copolymers. Unlike in other systems that contain non-ionic segments, the critical solution temperature of the polymers in the proposed system, which contains two polyampholyte segments, can be changed by changing the various parameters of the graft copolymers. Moreover, the easy tunability can potentially allow these graft copolymers to be used in a variety of applications, such as in sensitivity-tunable sensors or in the design of thermo optical devices. Further, these polymers can be easily transformed into multi-stimuli-responsive self-assembled nanogels, micelles, or other types of vesicles to enable controlled release of proteins. Additionally, the ability to load and

release proteins by changing the environmental conditions and enabling protection under severe stress can allow them to be used for the prevention or treatment of many neurodegenerative diseases. A direct extension of this study would be to study the controlled release of other biologically relevant proteins as protein drugs or as antimicrobial peptides. Research on utilizing the dual-thermo responsive property of such polymers for the release of drugs and proteins by changing the polymer architecture and composition is underway.

ASSOCIATED CONTENT

Supporting Information ^{1}H NMR spectrum of PLLSA, ^{1}H NMR spectrum of Macro-CTA, ^{1}H NMR and ^{13}C NMR spectrum of P1, ^{1}H NMR and ^{13}C NMR spectrum of P2, and time dependent ^{1}H NMR of P1 and P2, phase diagrams of homopolymers, and turbidity curve showing hysteresis of P1, and TEM images of P1 and P2, and images showing P2 and lysozyme hybrid formation.

AUTHOR INFORMATION

Corresponding Author

*Email: mkazuaki@jaist.ac.jp

ORCID

Kazuaki Matsumura: 0000-0001-9484-3073

Robin Rajan: 0000-0002-6610-9661

Notes

The authors declare no competing financial interests.

ACKNOWLEDGMENT

The authors thank Mrs. Keiko Kawamoto, Japan Advanced Institute of Science and Technology, for assistance in Cytotoxicity Assay and Mr. Harit Pitakjakpipop, Japan Advanced Institute of Science and Technology, for assistance in the taking of protein aggregation inhibition photographs.

Table of contents figure;

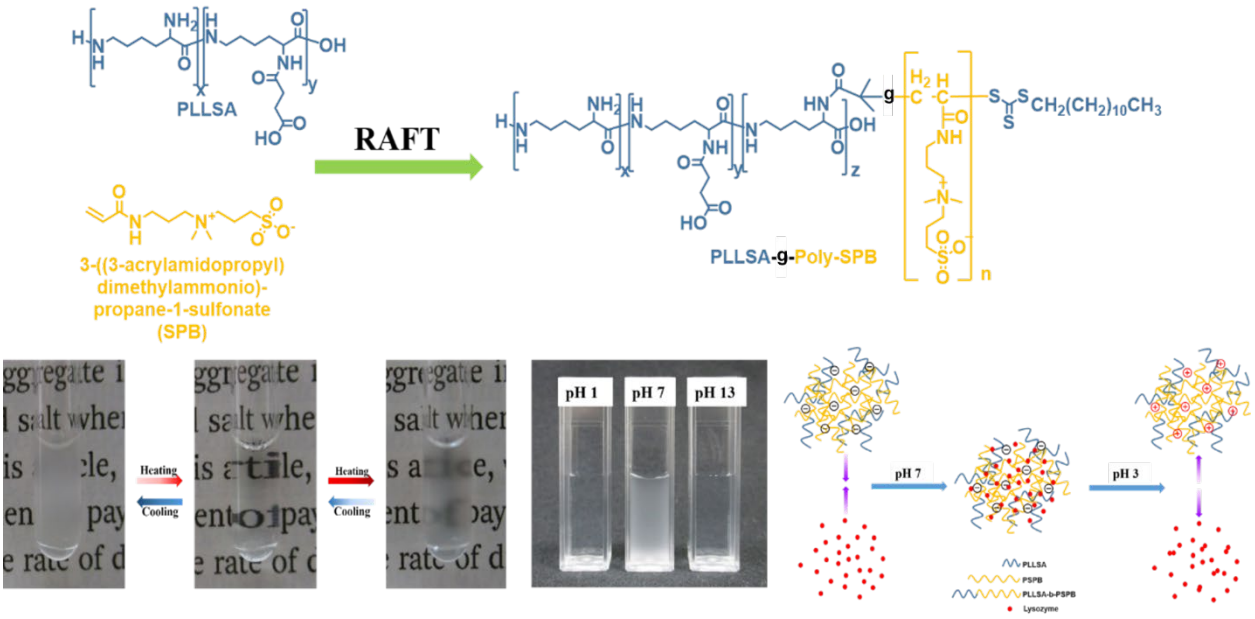

REFERENCES

(1) Ariga, K.; Kawakami, K.; Ebara, M.; Kotsuchibashi, Y.; Ji, Q.; Hill, J. P. Bioinspired Nanoarchitectonics as Emerging Drug Delivery Systems. *New J. Chem.* **2014**, *38* (11), 5149–5163.

(2) Aghabegi Moghanjoughi, A.; Khoshnevis, D.; Zarrabi, A. A Concise Review on Smart Polymers for Controlled Drug Release. *Drug Deliv. Transl. Res.* **2016**, *6* (3), 333–340.

(3) Jung, Y. seok; Park, W.; Park, H.; Lee, D. K.; Na, K. Thermo-Sensitive Injectable Hydrogel Based on the Physical Mixing of Hyaluronic Acid and Pluronic F-127 for Sustained NSAID Delivery. *Carbohydr. Polym.* **2017**, *156*, 403–408.

(4) Wang, G.; Nie, Q.; Zang, C.; Zhang, B.; Zhu, Q.; Luo, G.; Wang, S. Self-Assembled Thermoresponsive Nanogels Prepared by Reverse Micelle → Positive Micelle Method for Ophthalmic Delivery of Muscone, a Poorly Water-Soluble Drug. *J. Pharm. Sci.* **2016**, *105* (9), 2752–2759.

(5) Madhusudana Rao, K.; Mallikarjuna, B.; Krishna Rao, K. S. V.; Siraj, S.; Chowdoji Rao, K.; Subha, M. C. S. Novel Thermo/PH Sensitive Nanogels Composed from Poly(N-Vinylcaprolactam) for Controlled Release of an Anticancer Drug. *Colloids Surfaces B Biointerfaces* **2013**, *102*, 891–897.

(6) Shen, Y.; Li, G.; Ma, Y.; Yu, D.; Sun, J.; Li, Z. Smart Surfaces Based on Thermo-Responsive Polymer Brushes Prepared from l-Alanine Derivatives for Cell Capture and Release. *Soft Matter* **2015**, *11* (38), 7502–7506.

(7) Ebara, M.; Akimoto, M.; Uto, K.; Shiba, K.; Yoshikawa, G.; Aoyagi, T. Focus on the Interlude between Topographic Transition and Cell Response on Shape-Memory Surfaces. *Polymer (Guildf).* **2014**, *55* (23), 5961–5968.

(8) Mosqueira, D.; Pagliari, S.; Uto, K.; Ebara, M.; Romanazzo, S.; Escobedo-Lucea, C.; Nakanishi, J.; Taniguchi, A.; Franzese, O.; Di Nardo, P.; Goumans, M. J.; Traversa, E.; Pinto-do-Ó, P.; Aoyagi, T.; Forte, G. Hippo Pathway Effectors Control Cardiac Progenitor Cell Fate by Acting as Dynamic Sensors of Substrate Mechanics and Nanostructure. *ACS Nano* **2014**, *8* (3), 2033–2047.

(9) Kim, Y. J.; Kim, S. H.; Fujii, T.; Matsunaga, Y. T. Dual Stimuli-Responsive Smart Beads That Allow "on-off" Manipulation of Cancer Cells. *Biomater. Sci.* **2016**, *4* (6), 953–957.

(10) Paulus, A. S.; Heinzler, R.; Ooi, H. W.; Franzreb, M. Temperature-Switchable Agglomeration of Magnetic Particles Designed for Continuous Separation Processes in Biotechnology. *ACS Appl. Mater. Interfaces* **2015**, *7* (26), 14279–14287.

(11) Yoshimatsu, K.; Lesel, B. K.; Yonamine, Y.; Beierle, J. M.; Hoshino, Y.; Shea, K. J. Temperature-Responsive "Catch and Release" of Proteins by Using Multifunctional Polymer-Based Nanoparticles. *Angew. Chemie - Int. Ed.* **2012**, *51* (10), 2405–2408.

(12) Klaikherd, A.; Nagamani, C.; Thayumanavan, S. Multi-Stimuli Sensitive Amphilic Block Copolymer Assemblies. *J. Am. Chem. Soc.* **2009**, *131* (13), 4830–4838.

(13) Song, Z.; Wang, K.; Gao, C.; Wang, S.; Zhang, W. A New Thermo-, PH-, and CO 2 -Responsive Homopolymer of Poly[N-[2-(Diethylamino)Ethyl]Acrylamide]: Is the Diethylamino Group Underestimated? *Macromolecules* **2016**, *49* (1), 162–171.

(14) Ganesh, V. A.; Baji, A.; Ramakrishna, S. Smart Functional Polymers - A New Route towards Creating a Sustainable Environment. *RSC Adv.* **2014**, *4* (95), 53352–53364.

(15) Fournier, D.; Hoogenboom, R.; Thijs, H. M. L.; Paulus, R. M.; Schubert, U. S. Tunable PH- and Temperature-Sensitive Copolymer Libraries by Reversible Addition-Fragmentation Chain Transfer Copolymerizations of Methacrylates. *Macromolecules* **2007**, *40* (4), 915–920.

(16) Guragain, S.; Bastakoti, B. P.; Malgras, V.; Nakashima, K.; Yamauchi, Y. Multi-Stimuli-Responsive Polymeric Materials. *Chem. - A Eur. J.* **2015**, *21* (38), 13164–13174.

(17) Rajan, R.; Matsumura, K. Tunable Dual-Thermoresponsive Core–Shell Nanogels Exhibiting UCST and LCST Behavior. *Macromol. Rapid Commun.* **2017**, *38* (22) 1700478.

(18) Vishnevetskaya, N. S.; Hildebrand, V.; Niebuur, B.; Grillo, I.; Filippov, S. K.; Laschewsky, A.; Mu, P.; Papadakis, C. M. Aggregation Behavior of Doubly Thermoresponsive Polysulfobetaine - b - Poly(N - Isopropylacrylamide) Diblock Copolymers. *Macromolecules*, **2016,** 49, 6655–6668.

(19) Vishnevetskaya, N. S.; Hildebrand, V.; Dyakonova, M. A.; Niebuur, B.; Kyriakos, K.; Raftopoulos, K. N.; Di, Z.; Mu, P.; Laschewsky, A.; Papadakis, C. M. Dual Orthogonal Switching of the " Schizophrenic " Self-Assembly of Diblock Copolymers. *Macromolecules*, **2018**, 51, 2604–2614.

(20) Vishnevetskaya, N. S.; Hildebrand, V.; Niebuur, B.; Grillo, I.; Filippov, S. K.; Laschewsky, A.; Mu, P.; Papadakis, C. M. " Schizophrenic " Micelles from Doubly Thermoresponsive Polysulfobetaine - b - Poly(N - Isopropylmethacrylamide) Diblock Copolymers. *Macromolecules*, **2017**, 50, 3985–3999.

(21) Bromberg, L.; Levin, G. Poly(Amino Acid)-b-Poly(N,N-Diethylacrylamide)-b-Poly(Amino Acid) Conjugates of Well-Defined Structure. *Bioconjug. Chem.* **1998**, *9* (1), 40–49.

(22) Kim, S. W.; Jeong, B.; Bae, Y. H.; Lee, D. S. Biodegradable Block Copolymers as Injectable Drug-Delivery Systems. *Nature* **1997**, *388* (6645), 860–862.

(23) Furyk, S.; Zhang, Y.; Ortiz-Acosta, D.; Cremer, P. S.; Bergbreiter, D. E. Effects of End Group Polarity and Molecular Weight on the Lower Critical Solution Temperature of Poly(N-Isopropylacrylamide). *J. Polym. Sci. Part A Polym. Chem.* **2006**, *44* (4), 1492–1501.

(24) Das, E.; Matsumura, K. Tunable Phase-Separation Behavior of Thermoresponsive Polyampholytes through Molecular Design. *J. Polym. Sci. Part A Polym. Chem.* **2017**, *55* (5), 876–884.

(25) Wang, Y. W.; Chen, L. Y.; An, F. P.; Chang, M. Q.; Song, H. B. A Novel Polysaccharide Gel Bead Enabled Oral Enzyme Delivery with Sustained Release in Small Intestine. *Food Hydrocoll.* **2018**, *84* (November 2017), 68–74.

(26) Shih, I. L.; Shen, M. H.; Van, Y. T. Microbial Synthesis of Poly(ε-Lysine) and Its Various Applications. *Bioresour. Technol.* **2006**, *97* (9), 1148–1159.

(27) Matsumura, K.; Hyon, S. H. Polyampholytes as Low Toxic Efficient Cryoprotective Agents with Antifreeze Protein Properties. *Biomaterials* **2009**, *30* (27), 4842–4849.

(28) Zhang, W.; Yang, Z.; Kaufman, Y.; Bernstein, R. Surface and Anti-Fouling Properties of a Polyampholyte Hydrogel Grafted onto a Polyethersulfone Membrane. *J. Colloid Interface Sci.* **2018**, *517*, 155–165.

(29) Zhang, W.; Cheng, W.; Ziemann, E.; Be'er, A.; Lu, X.; Elimelech, M.; Bernstein, R. Functionalization of Ultrafiltration Membrane with Polyampholyte Hydrogel and Graphene Oxide to Achieve Dual Antifouling and Antibacterial Properties. *J. Memb. Sci.* **2018**, *565* (August), 293–302.

(30) Ahmed, S.; Hayashi, F.; Nagashima, T.; Matsumura, K. Protein Cytoplasmic Delivery Using Polyampholyte Nanoparticles and Freeze Concentration. *Biomaterials* **2014**, *35* (24), 6508–6518.

(31) Laschewsky, A. Structures and Synthesis of Zwitterionic Polymers. *Polymers (Basel).* **2014**, *6* (5), 1544–1601.

(32) Rajan, R.; Jain, M.; Matsumura, K. Cryoprotective Properties of Completely Synthetic Polyampholytes via Reversible Addition-Fragmentation Chain Transfer (RAFT) Polymerization and the Effects of Hydrophobicity. *J. Biomater. Sci. Polym. Ed.* **2013**, *24* (15), 1767–1780.

(33) Lowe, A. B.; Vamvakaki, M.; Wassall, M. A.; Wong, L.; Billingham, N. C.; Armes, S. P.; Lloyd, A. W. Well-Defined Sulfobetaine-Based Statistical Copolymers as Potential Antibioadherent Coatings. *J. Biomed. Mater. Res.* **2000**, *52* (1), 88–94.

(34) Rajan, R.; Matsumura, K. A Zwitterionic Polymer as a Novel Inhibitor of Protein Aggregation. *J. Mater. Chem. B* **2015**, *3* (28), 5683–5689.

(35) Rajan, R.; Matsumura, K. Inhibition of Protein Aggregation by Shell Nanogels. *Sci. Rep.* **2017**, No. March, 1–9.

(36) Rajan, R.; Suzuki, Y.; Matsumura, K. Zwitterionic Polymer Design That Inhibits Aggregation and Facilitates Insulin Refolding : Mechanistic Insights and Importance of Hydrophobicity. *Macromol. Biosci.* **2018**, *1800016*, 1–6.

(37) He, N.; Lu, Z.; Zhao, W. PH-Responsive Double Hydrophilic Protein-Polymer Hybrids and Their Self-Assembly in Aqueous Solution. *Colloid Polym. Sci.* **2015**, *293* (12), 3517–3526.

(38) Cao, Q.; He, N.; Wang, Y.; Lu, Z. Self-Assembled Nanostructures from Amphiphilic Globular Protein–Polymer Hybrids. *Polym. Bull.* **2018**, *75* (6), 2627–2639.

(39) Ge, J.; Neofytou, E.; Lei, J.; Beygui, R. E.; Zare, R. N. Protein-Polymer Hybrid Nanoparticles for Drug Delivery. *Small* **2012**, *8* (23), 3573–3578.

(40) Wu, C.; Baldursdottir, S.; Yang, M.; Mu, H. Lipid and PLGA Hybrid Microparticles as Carriers for Protein Delivery. *J. Drug Deliv. Sci. Technol.* **2018**, *43*, 65–72.

(41) Liu, Z.; Dong, C.; Wang, X.; Wang, H.; Li, W.; Tan, J.; Chang, J. Self-Assembled Biodegradable Protein-Polymer Vesicle as a Tumor-Targeted Nanocarrier. *ACS Appl. Mater. Interfaces* **2014**, *6* (4), 2393–2400.

(42) Matsudo, T.; Ogawa, K.; Kokufuta, E. Complex Formation of Protein with Different Water-Soluble Synthetic Polymers. *Biomacromolecules* **2003**, *4* (6), 1794–1799.

(43) Sandanaraj, B. S.; Vutukuri, D. R.; Simard, J. M.; Klaikherd, A.; Hong, R.; Rotello, V. M.; Thayumanavan, S. Noncovalent Modification of Chymotrypsin Surface Using an Amphiphilic Polymer Scaffold: Implications in Modulating Protein Function. *J. Am. Chem. Soc.* **2005**, *127* (30), 10693–10698.

(44) Jiang, Y.; Lu, H.; Yee Khine, Y.; Dag, A.; H. Stenzel, M. Polyion Complex Micelle Based on Albumin–Polymer Conjugates: Multifunctional Oligonucleotide Transfection Vectors for Anticancer Chemotherapeutics. *Biomacromolecules* **2014**, *15* (11), 4195–4205.

(45) Kao, C. H.; Wang, J. Y.; Chuang, K. H.; Chuang, C. H.; Cheng, T. C.; Hsieh, Y. C.; Tseng, Y. long; Chen, B. M.; Roffler, S. R.; Cheng, T. L. One-Step Mixing with Humanized Anti-MPEG Bispecific Antibody Enhances Tumor Accumulation and Therapeutic Efficacy of MPEGylated Nanoparticles. *Biomaterials* **2014**, *35* (37), 9930–9940.

(46) Habeeb, A. F. S. A. Determination of Free Amino Groups in Proteins by Trinitrobenzenesulfonic Acid. *Anal. Biochem.* **1966**, *14* (3), 328–336.

(47) Ismail, A. M. A Rapid and Sensitive Method for the Quantitation of Microgram Quantities of Protein Utilizing the Principle of Protein-Dye Binding. *Anal. Biochem.* **1976**, *72* (1–2), 248–254.

(48) Taneja, S.; Ahmad, F. Increased Thermal Stability of Proteins in the Presence of Amino Acids. *Biochem. J.* **1994**, *303*, 147–153.

(49) Seuring, J.; Agarwal, S. Polymers with Upper Critical Solution Temperature in Aqueous Solution. *Macromol. Rapid Commun.* **2012**, *33*, 1898–1920.

(50) Ghaderi, R.; Carlfors, J. Biological Activity of Lysozyme After Entrapment in Poly (d,l-Lactide-Co-Glycolide)-Microspheres. *Pharm. Res.* **1997**, *14* (11), 1556–1562.

(51) CANFIELD, R. E. The Amino Acid Sequence of Egg White Lysozyme. *J. Biol. Chem.* **1963**, *238* (8), 2698–2707.

(52) BLAKE, C. C. F.; KOENIG, D. F.; MAIR, G. A.; NORTH, A. C. T.; PHILLIPS, D. C.; SARMA, V. R. Structure of Hen Egg-White Lysozyme: A Three-Dimensional Fourier Synthesis at 2 Å Resolution. *Nature* **1965**, *206* (4986), 757–761.

(53) Lee, C.; Jeong, J.; Lee, T.; Zhang, W.; Xu, L.; Choi, J. E.; Park, J. H.; Song, J. K.; Jang, S.; Eom, C. Y.; Shim, K.; Seong, Soo. AA.; Kang, Y. S.; Kwak, M.; Jeon, H. J.; Go, J. S.; Suh, Y. D.; Jin, J. O.; Paik, H. J. Virus-Mimetic Polymer Nanoparticles Displaying Hemagglutinin as an Adjuvant-Free Influenza Vaccine. *Biomaterials* **2018**, *183* (July), 234–242.

(54) Lee, C.; Choi, J. E.; Park, G. Y.; Lee, T.; Kim, J.; An, S. S. A.; Song, J. K.; Paik, H. jong. Size-Tunable Protein–Polymer Hybrid Carrier for Cell Internalization. *React. Funct. Polym.* **2018**, *124* (September 2017), 72–76.

(55) Kadir, M. A.; Lee, C.; Han, H. S.; Kim, B. S.; Ha, E. J.; Jeong, J.; Song, J. K.; Lee, S. G.; An, S. S. A.; Paik, H. J. In Situ Formation of Polymer-Protein Hybrid Spherical Aggregates from (Nitrilotriacetic Acid)-End-Functionalized Polystyrenes and His-Tagged Proteins. *Polym. Chem.* **2013**, *4* (7), 2286–2292.

(56) Lee, C.; Jose, L.; Shim, K.; An, S. S. A.; Jang, S.; Song, J. K.; Jin, J.-O.; Paik, H. Influenza Mimetic Protein–Polymer Nanoparticles as Antigen Delivery Vehicles to Dendritic Cells for Cancer Immunotherapy. *Nanoscale* **2019**, *11* (29), 13878–13884.

(57) Sharma, N.; Rajan, R.; Makhaik, S.; Matsumura, K. Comparative Study of Protein Aggregation Arrest by Zwitterionic Polysulfobetaines : Using Contrasting Raft Agents. *ACS Omega* **2019**, *4*, 12186–12193.

(58) Muraoka, T.; Adachi, K.; Ui, M.; Kawasaki, S.; Sadhukhan, N.; Obara, H.; Tochio, H.; Shirakawa, M.; Kinbara, K. A Structured Monodisperse PEG for the Effective Suppression of Protein Aggregation. *Angew. Chemie - Int. Ed.* **2013**, *52* (9), 2430–2434.

(59) Whitmore, L.; Wallace, B. A. DICHROWEB, an Online Server for Protein Secondary Structure Analyses from Circular Dichroism Spectroscopic Data. *Nucleic Acids Res.* **2004**, *32* (WEB SERVER ISS.), 668–673.

(60) Sreerama, N.; Woody, R. W. Estimation of Protein Secondary Structure from Circular Dichroism Spectra: Comparison of CONTIN, SELCON, and CDSSTR Methods with an Expanded Reference Set. *Anal. Biochem.* **2000**, *287* (2), 252–260.

Supporting Information

Dual Thermo- and pH-responsive Behavior of Double Zwitterionic Graft Copolymers for Suppression of Protein Aggregation and Protein Release

Dandan Zhao[†], *Robin Rajan*[†] *and Kazuaki Matsumura* [*†]

† School of Materials Science, Japan Advanced Institute of Science and, Technology, 1-1 Asahidai, Nomi, Ishikawa 923-1292, Japan

Corresponding Author: Kazuaki Matsumura

Email: mkazuaki@jaist.ac.jp.

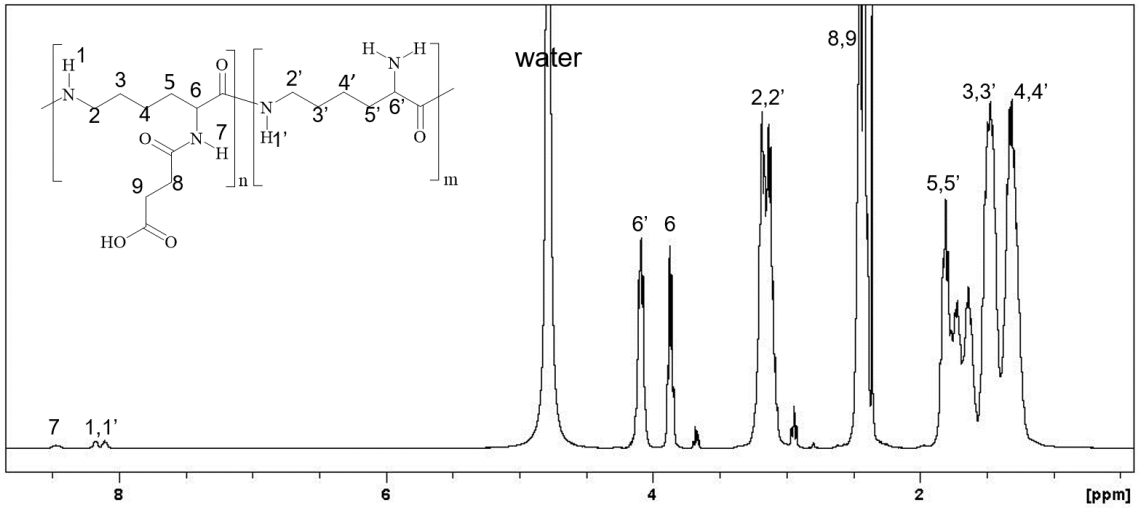

Figure S1. ^{1}H NMR of PLLSA in D_2O

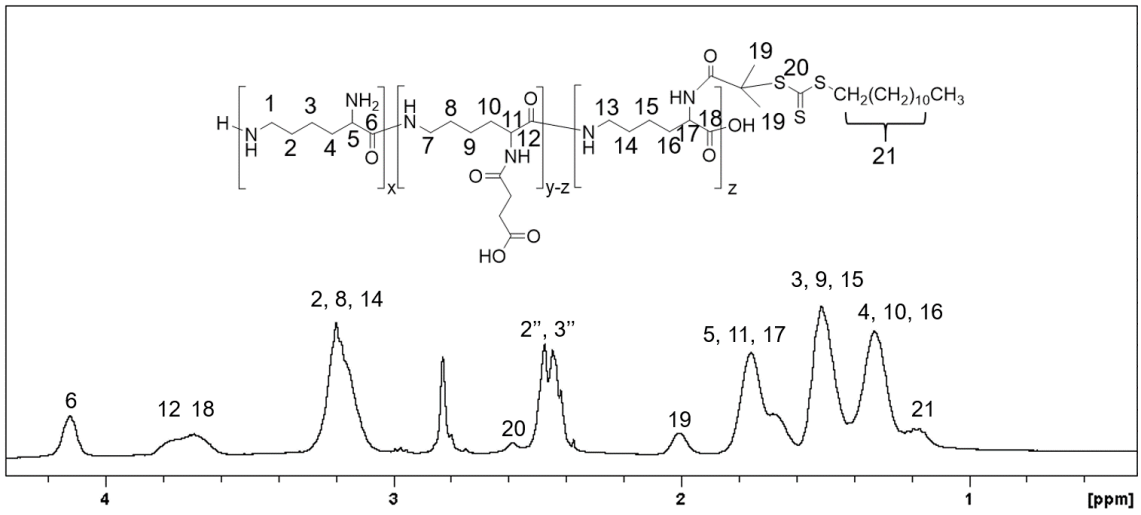

Figure S2. ^{1}H NMR of Macro-CTA in D_2O

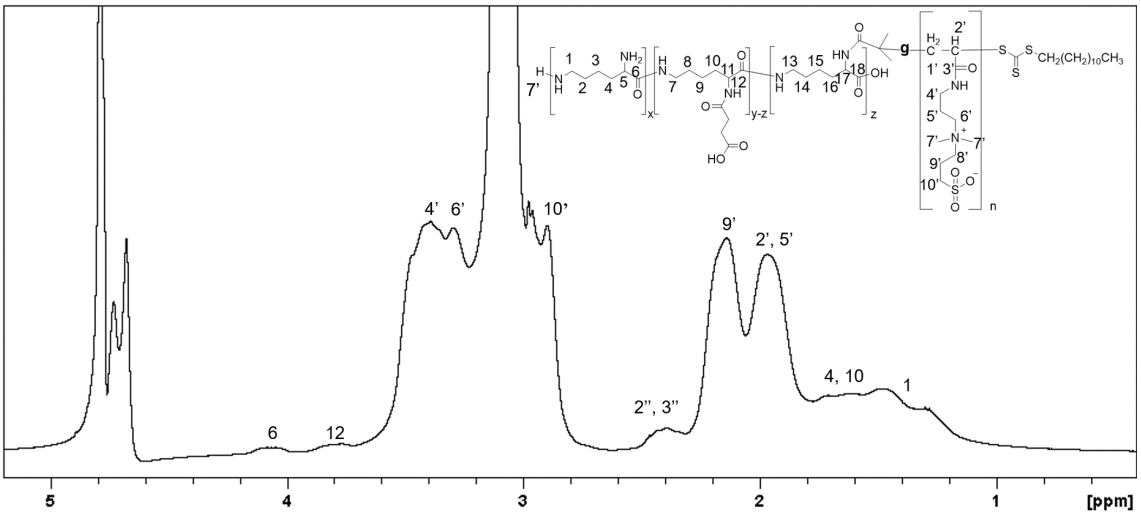

Figure S3. ^{1}H NMR of P1 in D_2O

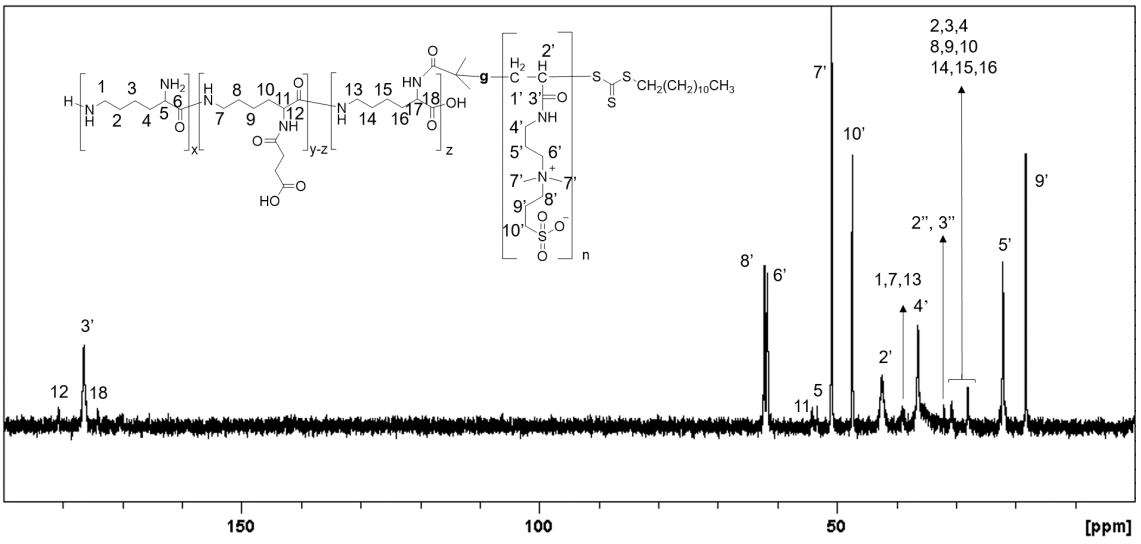

Figure S4. ^{13}C NMR of P1 in D_2O

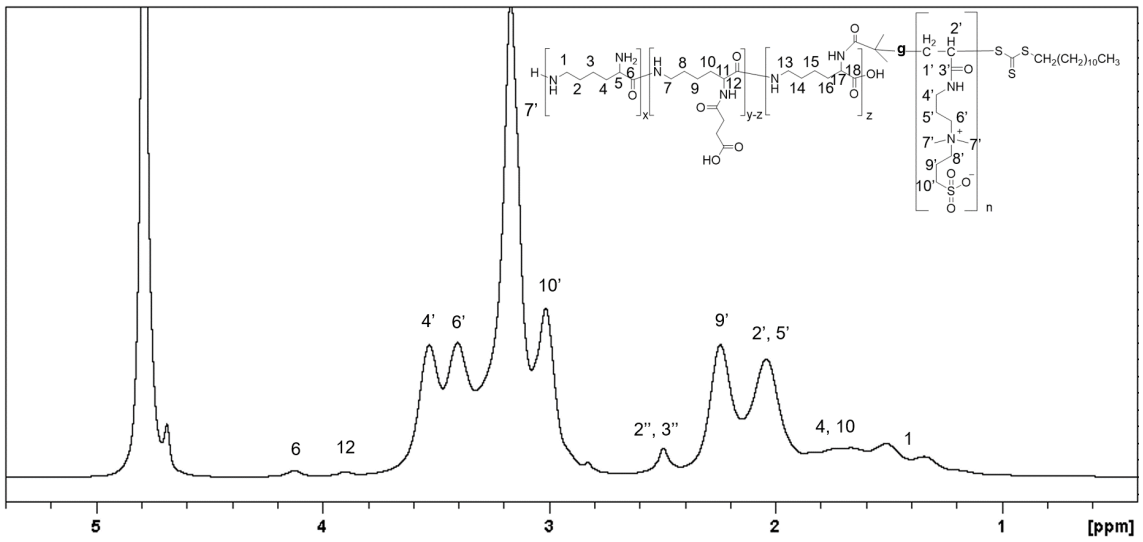

Figure S5. ^{1}H NMR of P2 in D_2O

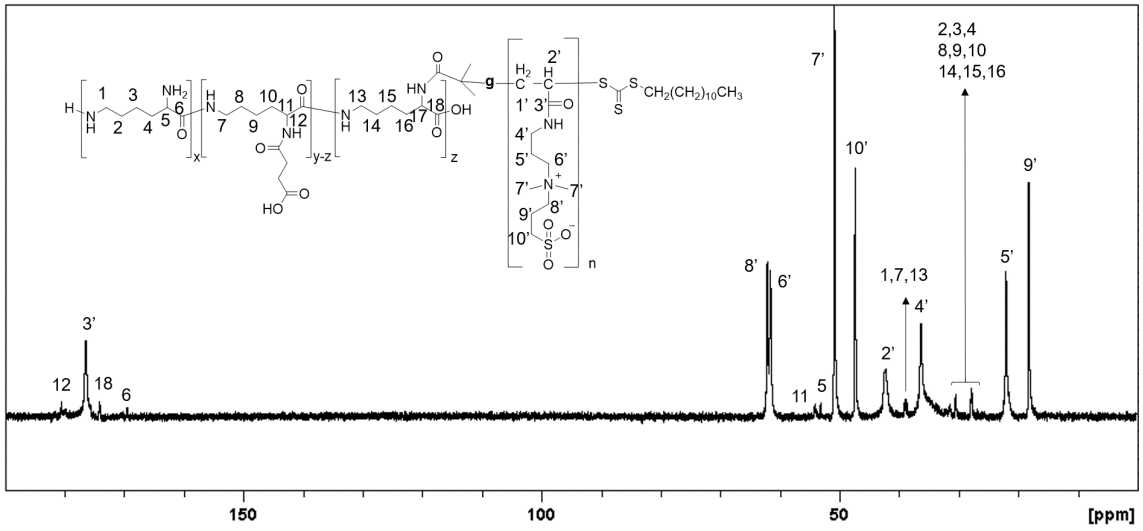

Figure S6. ^{13}C NMR of P2 in D_2O

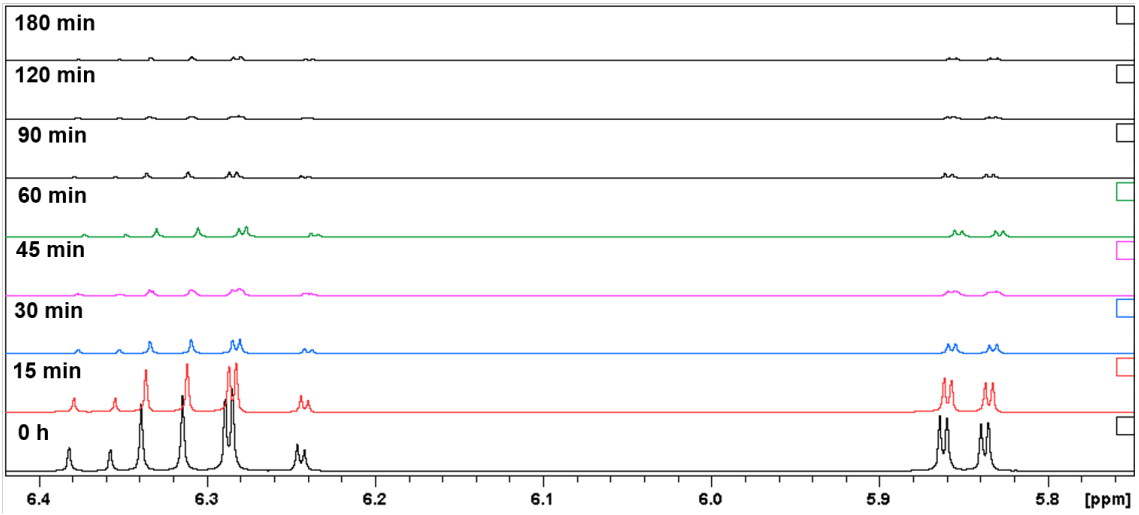

Figure S7. Time-dependent ^{1}H-NMR spectra of P1 in D_2O

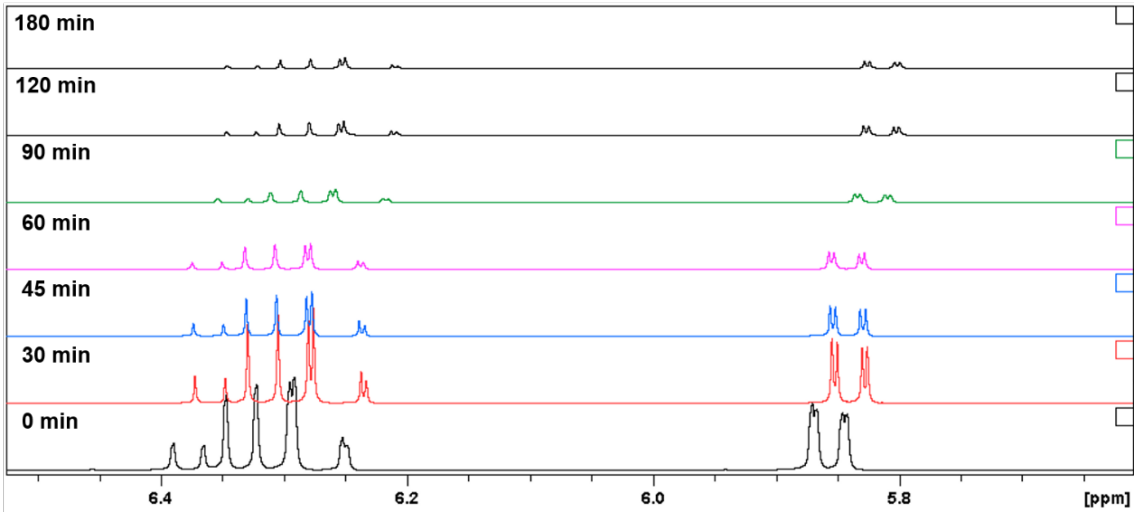

Figure S8. Time-dependent ^{1}H-NMR spectra of P2 in D_2O

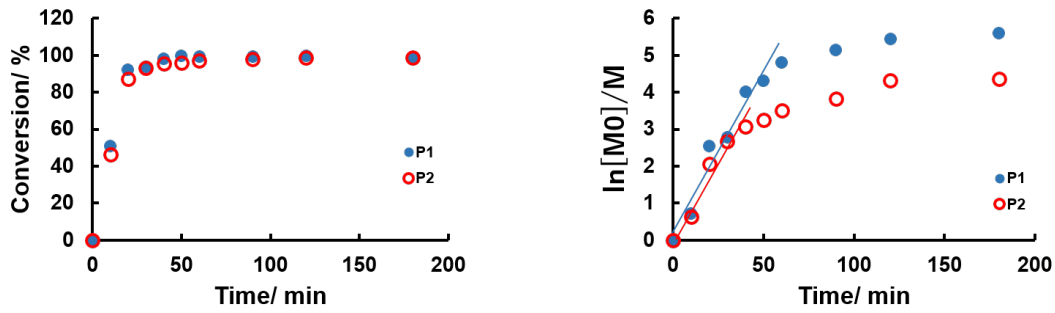

Figure S9. Kinetic plot showing the polymerization of the block copolymer.

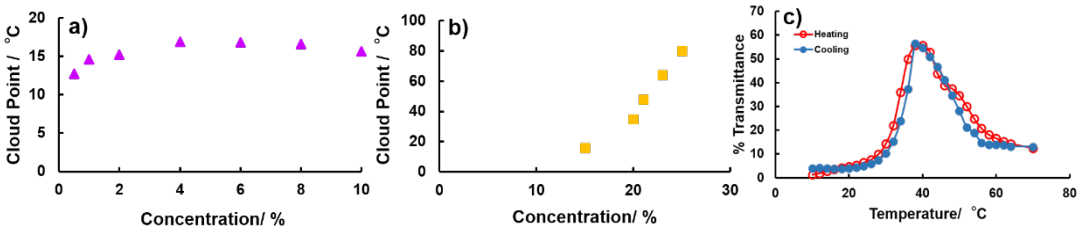

Figure S10. Phase diagrams of a) PSPB homopolymer solution and b) PLLSA50 polymer solution. c) Hysteresis curves of 2% (w/w) P1 in distilled water. Red line: heating; blue line: cooling.

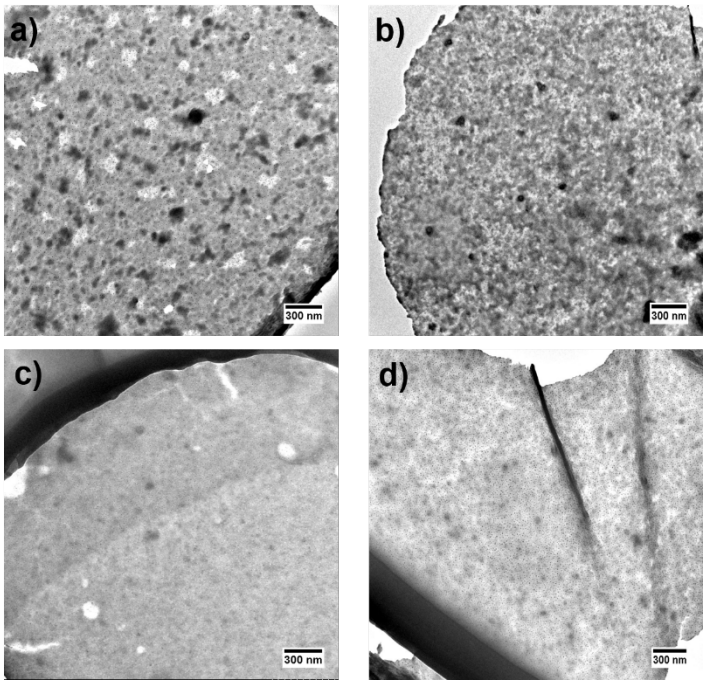

Figure S11. TEM image of P1 (a and b) and P2 (c and d) from a solution of concentration 0.1% at temperature 4 °C (a and c) and temperature 70 °C (b and d). Bars; 300 nm

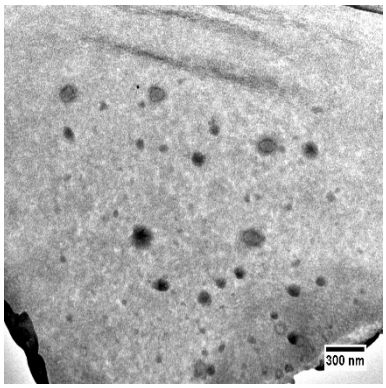

Figure S12. TEM image of P2-lysozyme hybrids. The concentrations of P2 and lysozyme were 5% (w/w) and 0.3% (w/w), respectively, in PBS (pH = 7.4) after heating at 90 °C for 30 min. Bar; 300 nm.